Assessing ADR's deep geothermal capabilities against Contact Energy's temperature logs in the Wairakei Geothermal Zone, New Zealand.

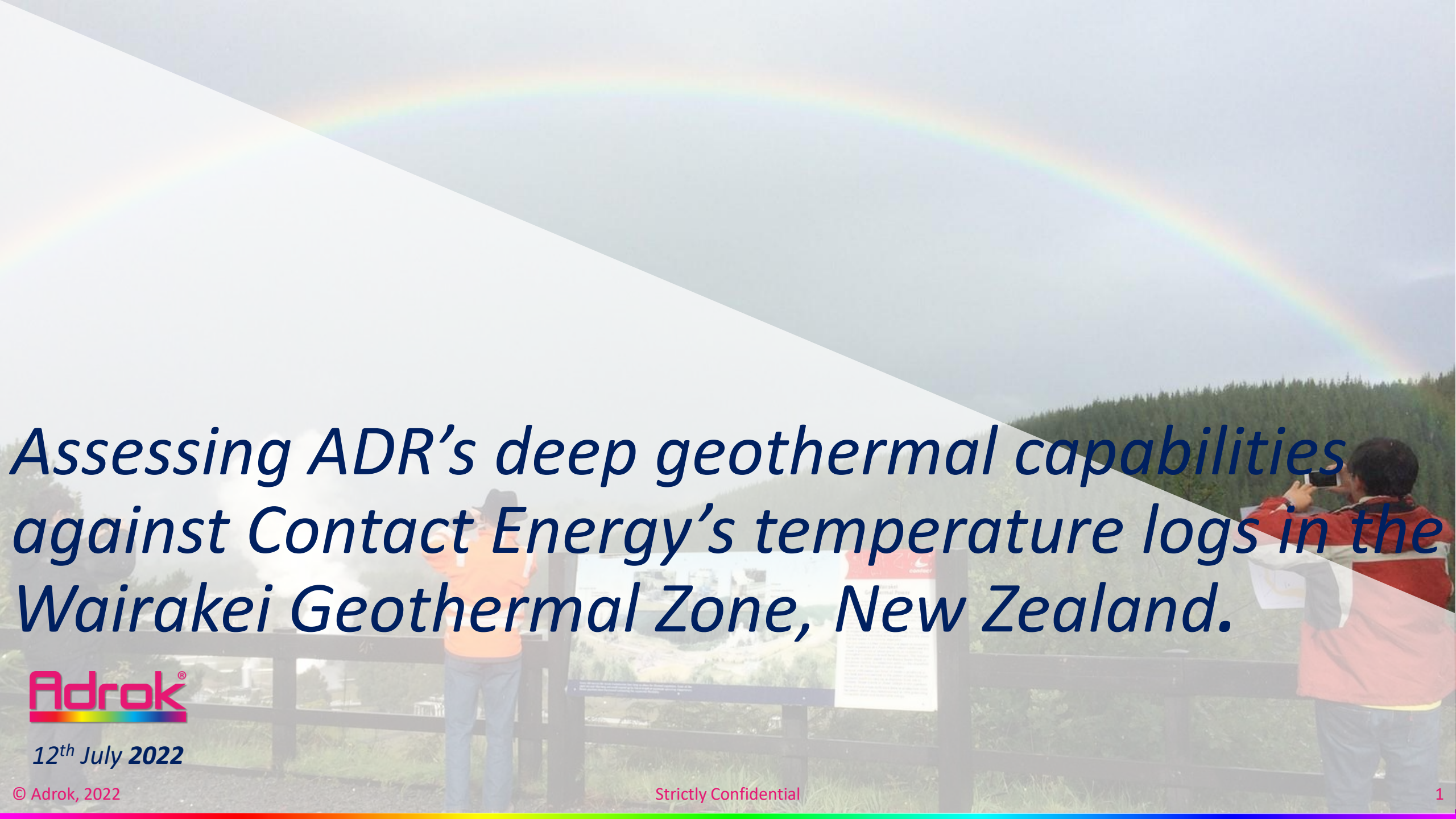

*12th July **2022***

Glossary

Term	Definition
Dielectric Constant	The index of the rate of transmission of our ADR wave packet through a medium relative to the transmission rate of the beam through vacuum. This is also sometimes called the transmissivity index, or relative permittivity. The vacuum has a dielectric constant of 1. For a medium such as limestone the dielectric constant (ϵr) is typically 9.
Energy-Gamma (E-Gamma)	Energy reflectivity measurement of a subsurface layer of measured thickness, commonly used in image processing under the name of modulation (see Mather and Koch, 2011).
Stare	A stationary scan where data collected with both antennae pointing the ground., including Harmonics, and Correlation as input
WARR	Wide Angle Reflection and Refraction scan to triangulate subsurface depths from the surface ground level. The Transmitting Antenna is moved at ground level along the scan line, away from the stationary Receiving Antenna which is fixed to the start of the scan line. Collected by ADR Scanner at ground level (that produces depth calculations).

The Problem

Trying to quantify subsurface rock, mineral, gas, fluid, density and temperature conditions for the exploration & production of natural resources is difficult because of the following reasons:

Subsurface fluids, porosity, permeability, minerals and temperature are very uncertain and difficult to read as they are dynamic and complex

The easiest way to read it accurately is through drilling which is very expensive & environmentally damaging

The Solution

Atomic Dielectric Resonance (ADR)

Using pulsed electromagnetic ADR Technology, we can now determine the existence of subsurface natural resources, movements and fluids without the need for invasive drilling

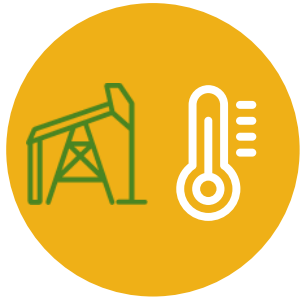

ADR allows the measurement of subsurface temperature, rock, mineral, fluid and gas conditions from the earth's surface, non-destructively

Our technology eliminates the need for drilling and therefore reduces the expense and risks associated with it

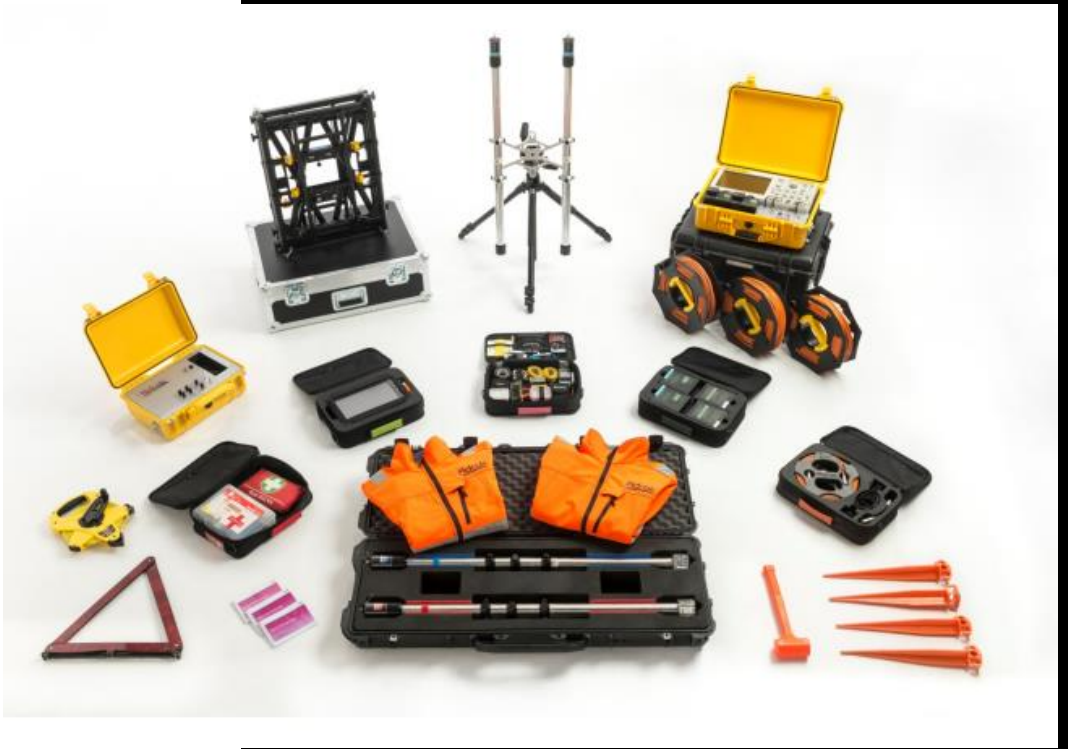

Locations

TH11	WK271
1 x Shallow Stare 1 x Deep Stare 1 x WARR	1 x Deep Stare 1 x WARR

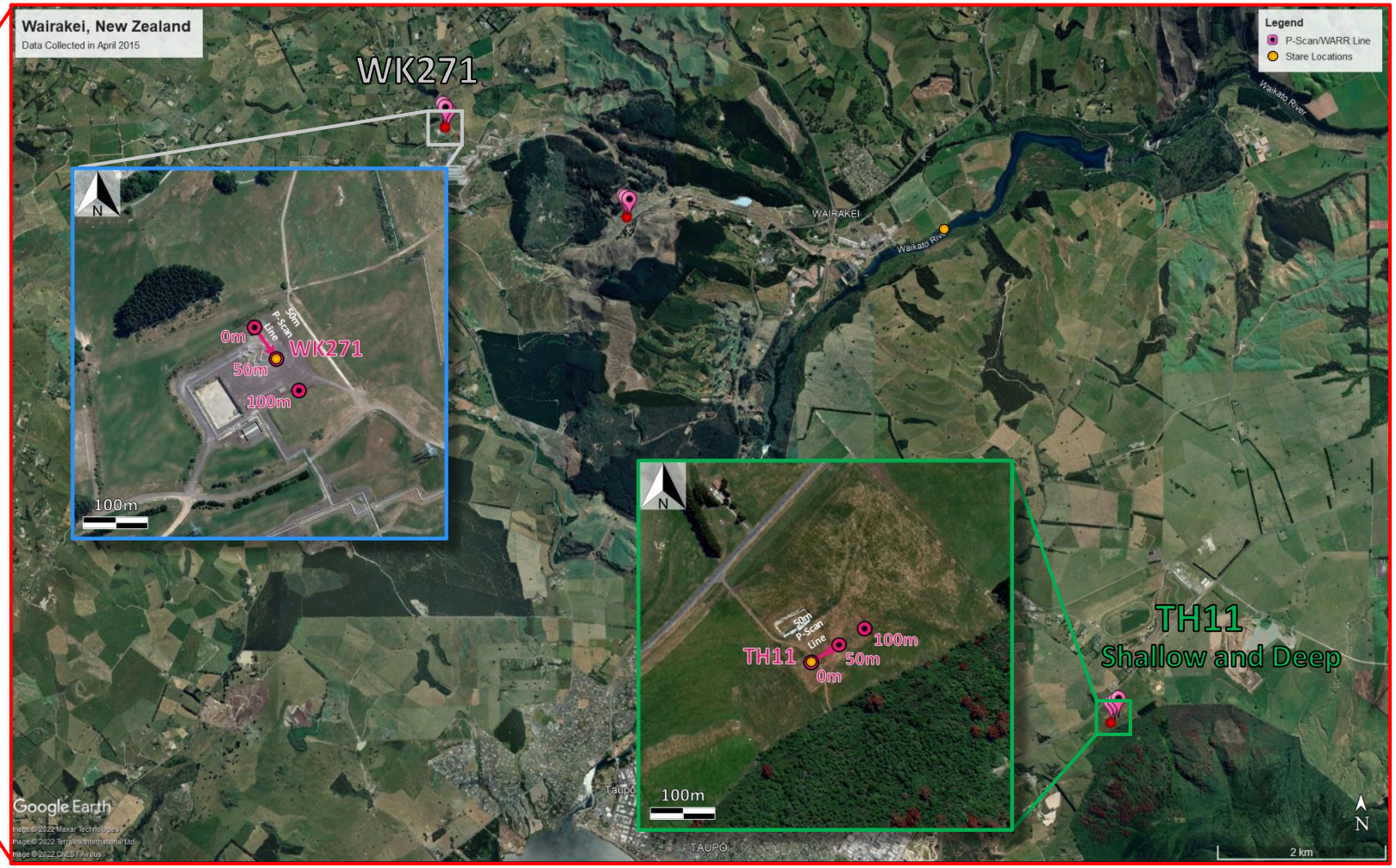

Methods E-Gamma Trough Analysis

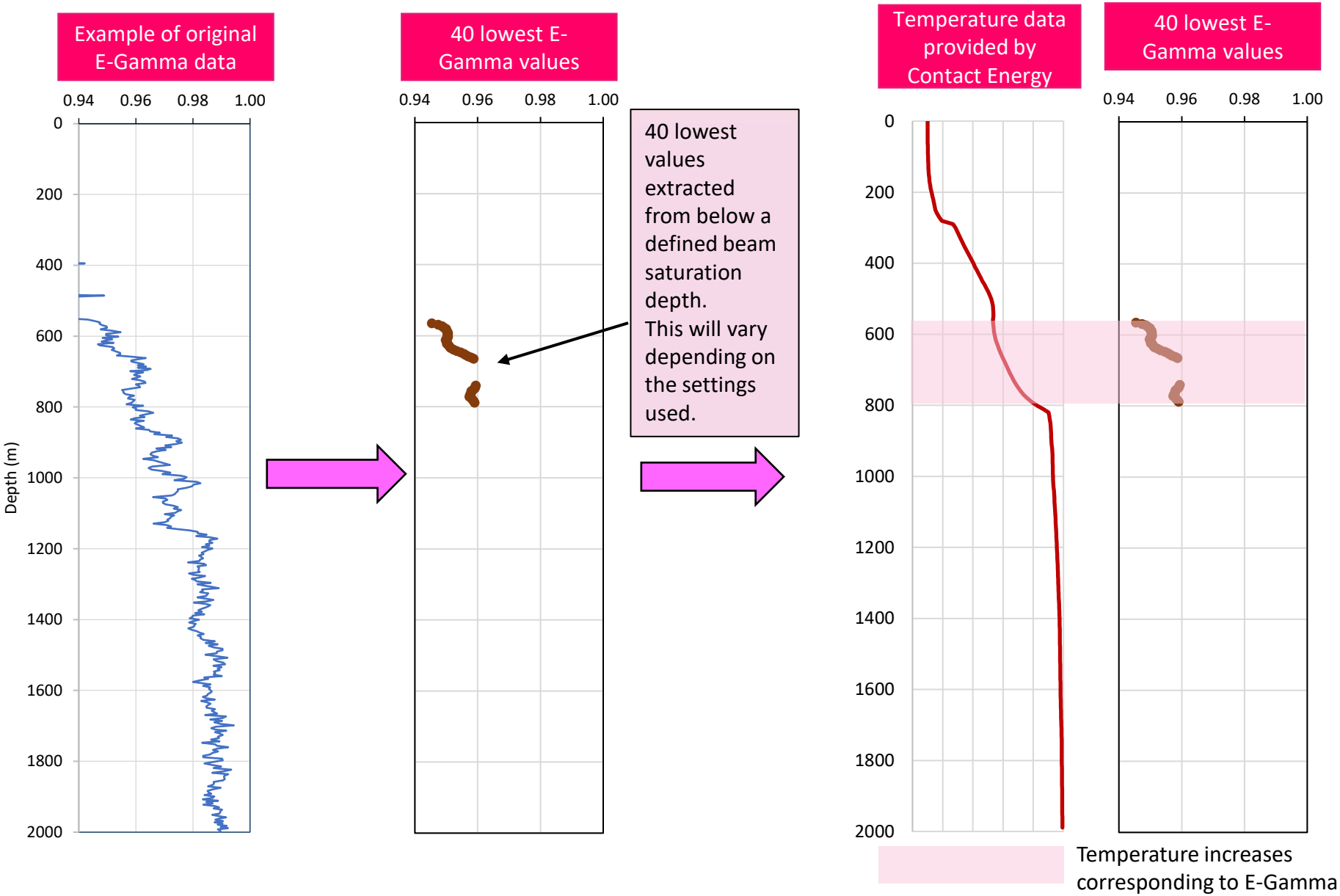

- The lowest 40 E-Gamma values are extracted from the full dataset after taking into account the beam saturation for both settings at TH11 and WK271. These values were then compared with the temperature data provided by Contact Energy.
- Areas where temperature increases correspond to the presence of E-Gamma troughs are highlighted.

Methods Dielectric Constant

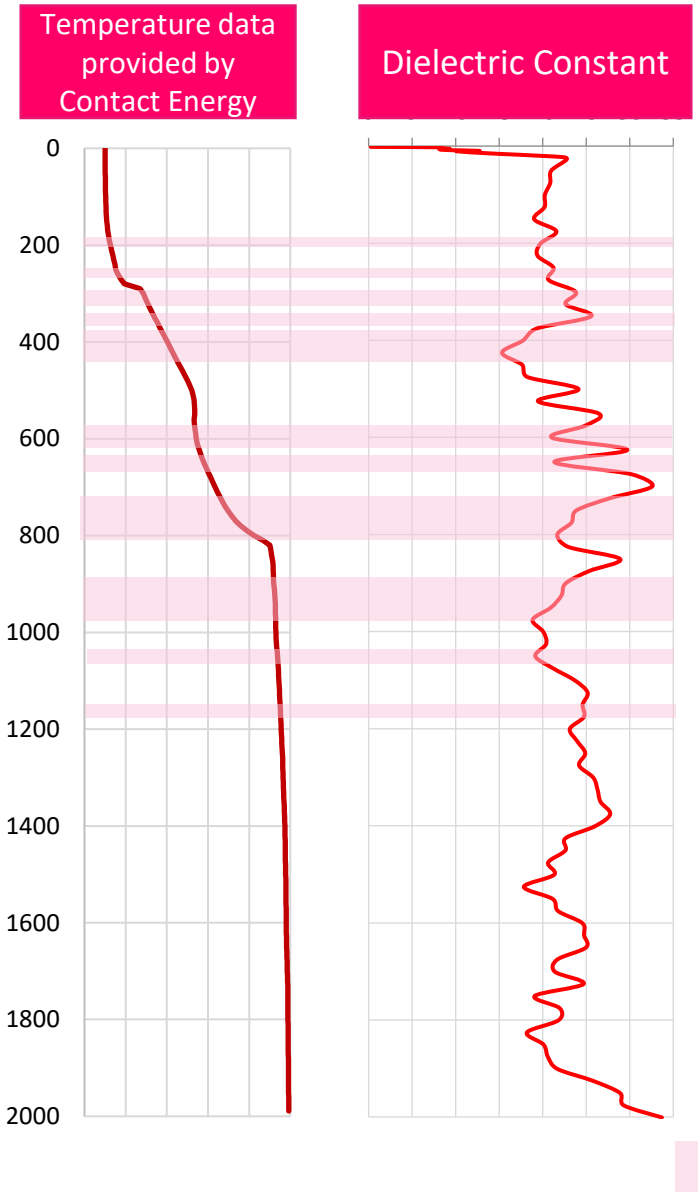

- The dielectric constant was calculated at regular equal depth intervals over the length and depth of the WARR scan.
- The troughs in the calculated dielectric constant were then compared with the temperature data provided by Contact Energy for each setting at TH11 and WK271. Lows in dielectric that correspond with increases in temperature are then highlighted
- These interpretations were then combined with the interpretations from the E-Gamma to assess how well ADR has identified these temperature increases.

Temperature increases corresponding to dielectric troughs.

TH11 SSET: E-Gamma and Dielectrics

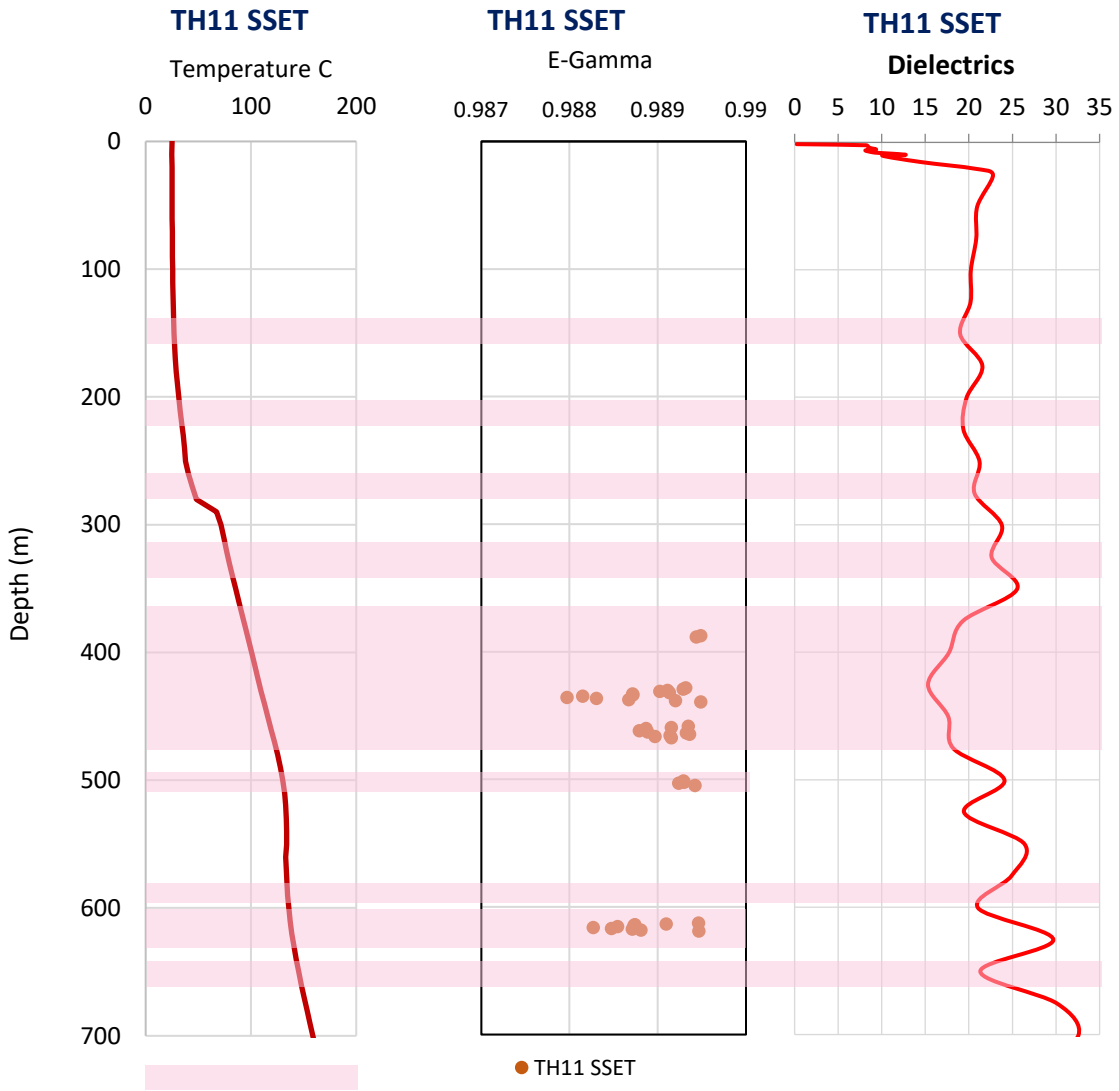

Temperature increases corresponding to E-Gamma and/or dielectric troughs.

- The lowest 40 E-Gamma values are extracted from the full dataset after taking into account the beam saturation and compared with the training data. Troughs in the dielectric constant that correspond to temperature increases are also highlighted.
- A continuous temperature increase of 67.5˚C -128.5˚C between 290m-500m is identified by the presence of the majority of 40 E-Gamma troughs and a broad trough in the dielectrics where values drop from 22 to 15 between 375m-480m.
- A further increase in temperature of 134.12˚C -156.06˚C from 590m-700m is captured by the presence of E-Gamma values between 600m-630m and two separate declines in the dielectric constant from 25 to 20 at both 590m and 660m.
- Troughs in the dielectric constant at 140m-160m, 200m-210m and 270-280m also correspond to temperature increases from 26.23˚C-27.02˚C, 31.48˚C-32.46˚C and 44.19˚C -48.23˚C.
- An increase in temperature from 128.13˚C to 130.24˚C is marked by the presence of three E-Gamma lows.
- The data for both parameters identifies multiple increases in temperature. The results **are good**.

TH11 DSET: E-Gamma and Dielectrics

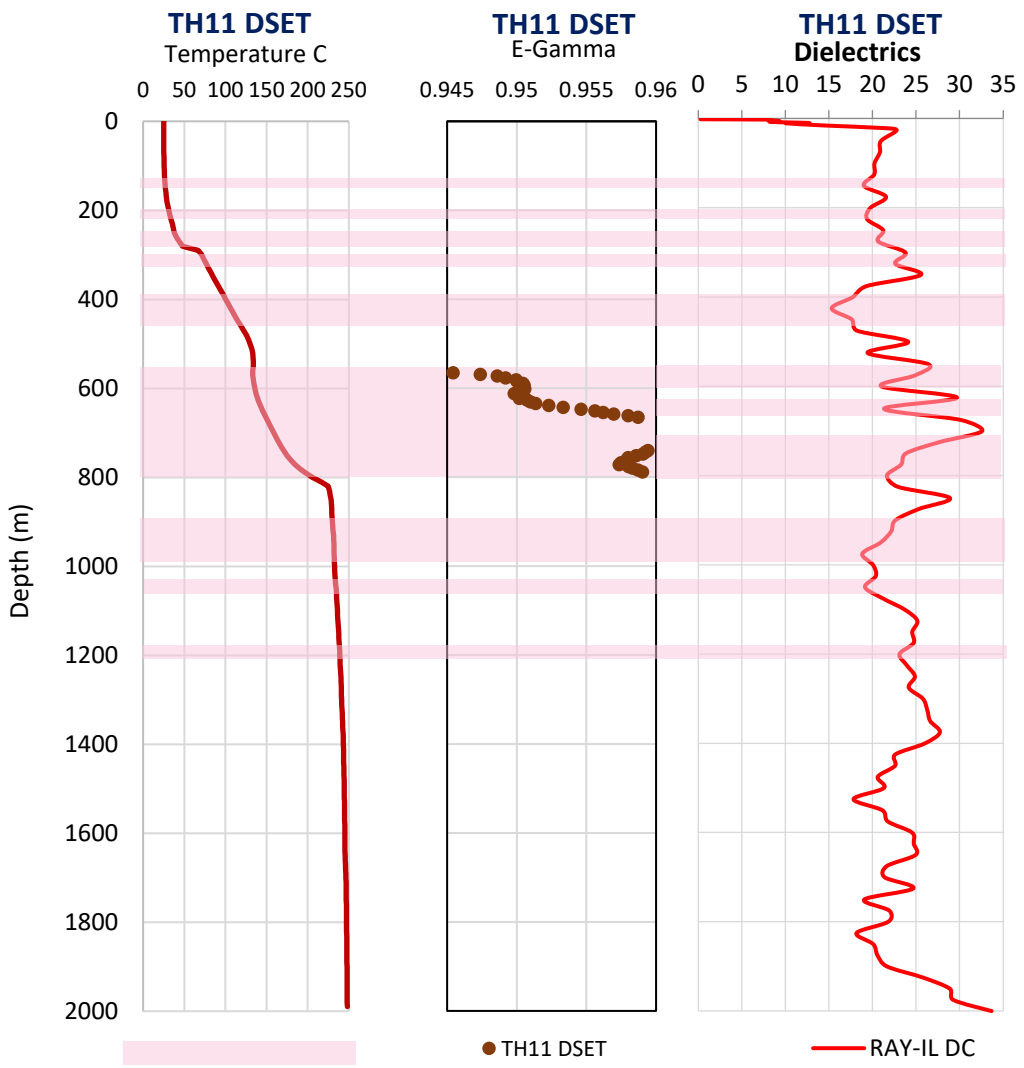

Temperature increases corresponding to E-Gamma and dielectric troughs.

- The lowest 40 E-Gamma values are extracted from the full dataset after taking into account the beam saturation and compared with the training data. Troughs in the dielectric constant that correspond to temperature increases are also highlighted.
- All 40 E-Gamma troughs correspond to the largest increase in temperature in the whole log. This occurs between 590-800m and a temperature increase from 134.85˚C to 206˚C. This is an increase in temperature of 68˚C over 210m.
- Low dielectrics corresponding to increasing temperature are seen between 200m-210m, 275m-295m, 300m-325m, 350m-420m, 590m-600m and 650m-660m, 700m-800m, 850m-990m, 1040m-1050m, 1190m-1200m. This means that both parameters identify the large temperature increase between 580m-800m.
- Furthermore the relative absence of troughs in both parameters below 1,000m where temperature increases are relatively small (~25˚C increase between 1000m-2000m) indicates an absence of false positives in this area.
- Larger and more regular troughs in both parameters are seen corresponding to the largest increase in temperature. This a **good result**.

WK271: E-Gamma and Dielectrics

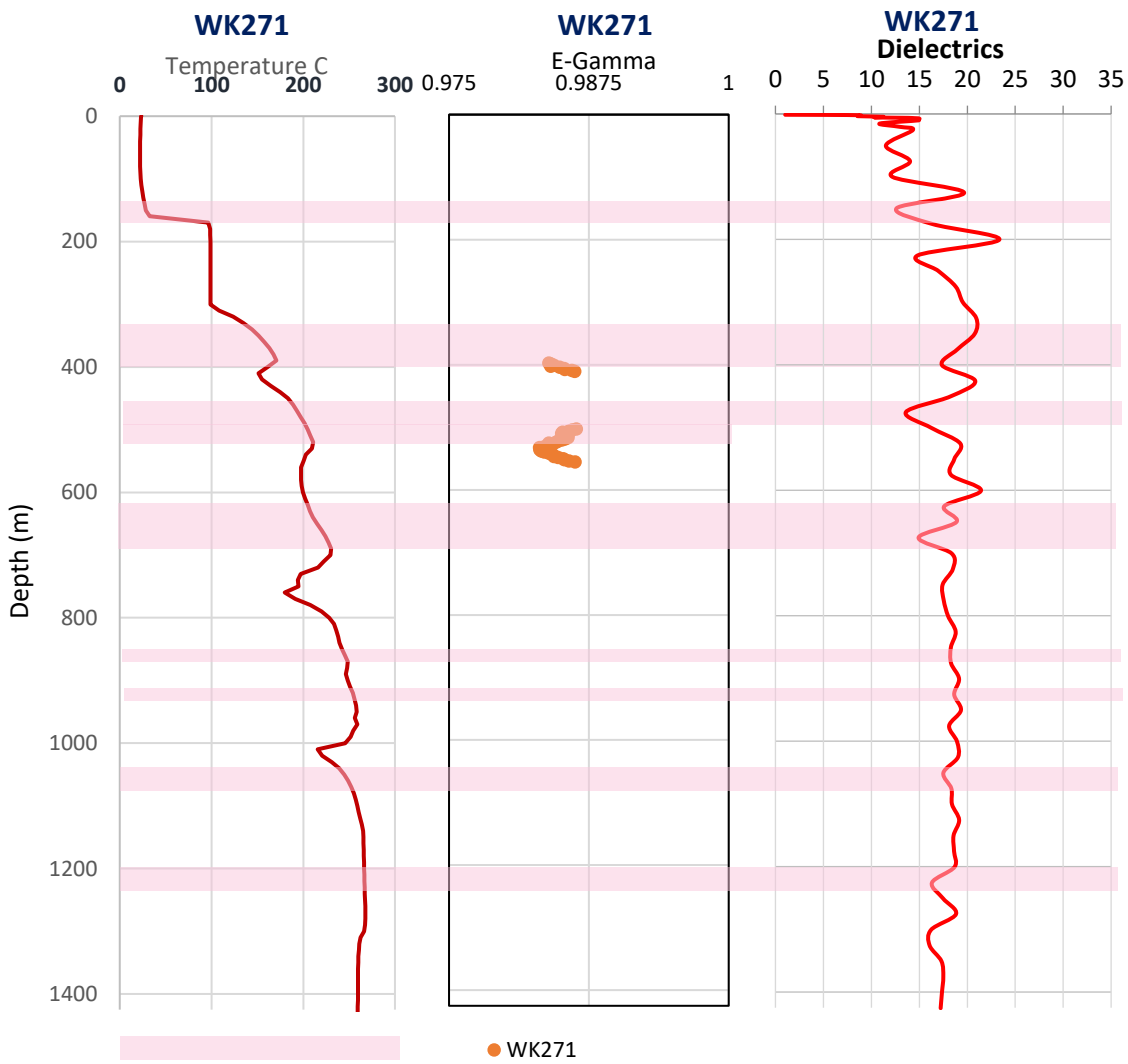

Temperature increases corresponding to E-Gamma and dielectric troughs.

- The lowest 40 E-Gamma values are extracted from the full dataset after taking into account the beam saturation and compared with the training data. These have been re-processed using different scans to enhance the results. Troughs in the dielectric constant that correspond to temperature increases are also highlighted.
- Four E-Gamma troughs are seen between 396m-402m, corresponding to a peak in temperature of 170.6˚C.
- Most of the 40 troughs correspond to a zone between 496-566m. E-Gamma values decrease from 496m-537m corresponding to an increase temperature values from 201˚C to 209˚C. An increase of 8˚C over 41m. However, the temperature increases between 620m-1000m are not seen in the lowest 40 E-Gamma values.
- Low dielectrics corresponding to increasing temperature are seen between 310m-390m, 425m-475m, 610m-700m, 840m-850m, 920m 930m, 1040m-1080m, 1200m-1240m.
- The dielectrics partially identifies all the increases in temperature while the E-Gamma troughs identifies two of the largest increases in temperature. This is a **good result**.

Raw data

- Simple ADR analysis is to plot the data stack versus depth
- Requires raw ADR data and DCO file for depthing
- ADR TRA depthin' program: tra2depth (MATLAB or EXE)
  - Produces MAT format ADR data with added field "depth"
- Next raw data plots of the 2 sites

TH11: Raw Data

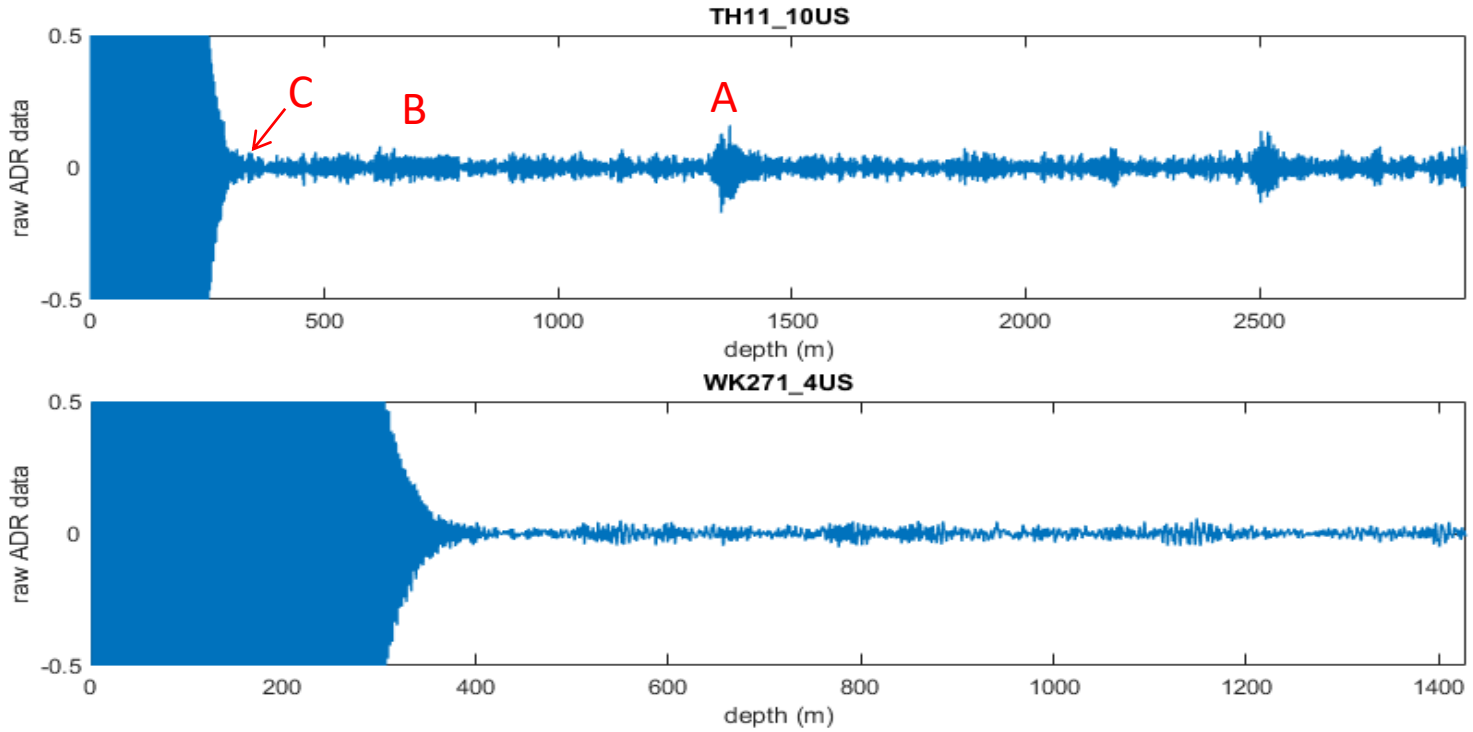

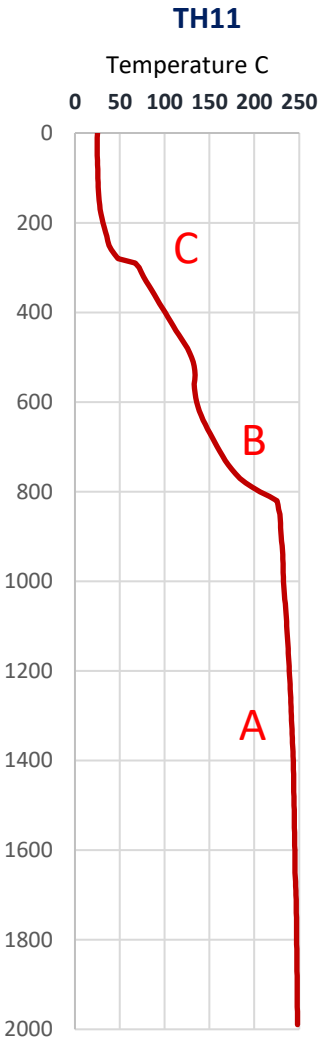

Most prominent ADR feature below 2200m is at 1320-1420m (A), which does not correspond with a temperature change. The B “burst” from 600-790m corresponds to a marked steep raise in temperature. The jump in temperature at 280m perhaps can be seen at C at 305m in the ADR plot, but it is too close to the saturation zone to be sure.

TH11: Correlation/entropy

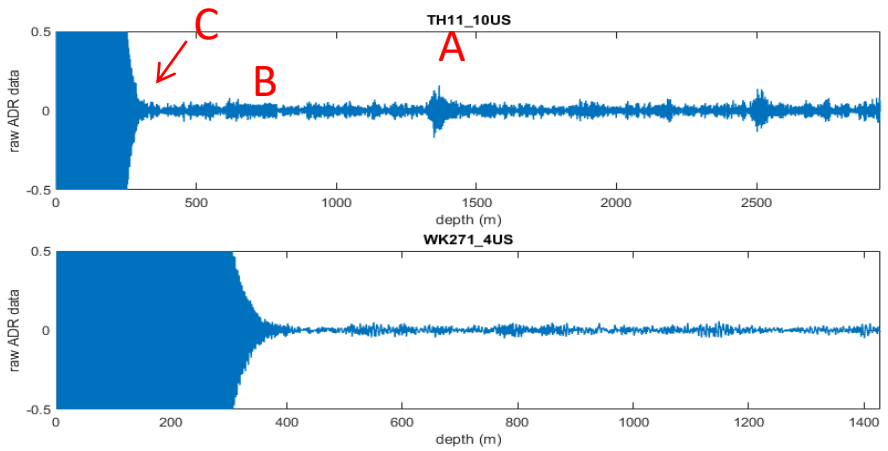

Most prominent ADR feature below 2200m is at 1320-1420m (A), which does not correspond with a temperature change. The B "burst" from 600-790m corresponds to a marked steep raise in temperature. The jump in temperature at 280m perhaps can be seen at C at 305m in the ADR plot, but it is too close to the saturation zone to be sure.

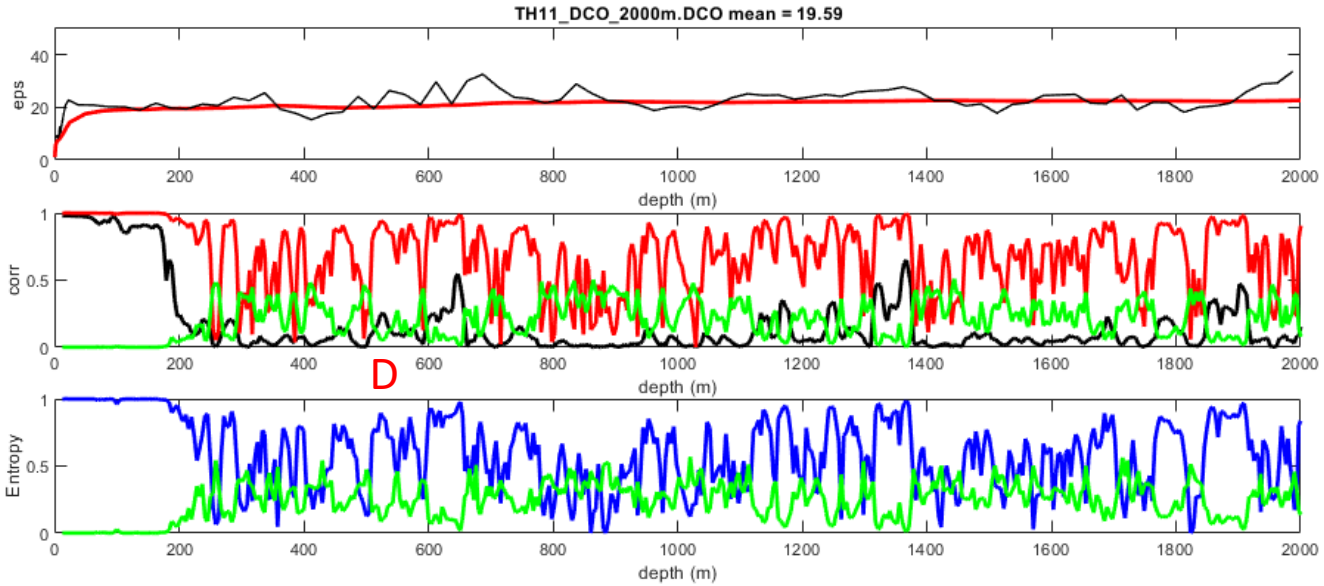

Correlation/entropy has many more peaks than usual. So much so that even the raw correlation (black curve) shows significant features whereas there is too much data in correlation and entropy. The two large peaks near 1400m and 600m (also strong dips in standard deviation (green)) are the features A and B, and feature C is also a clear peak (in black and red/blue). These peak support previous conclusion.
In addition the peak at 520m corresponds to the kink at "D" in temperature.
Other peaks in correlation/entropy seem unrelated to temperature.

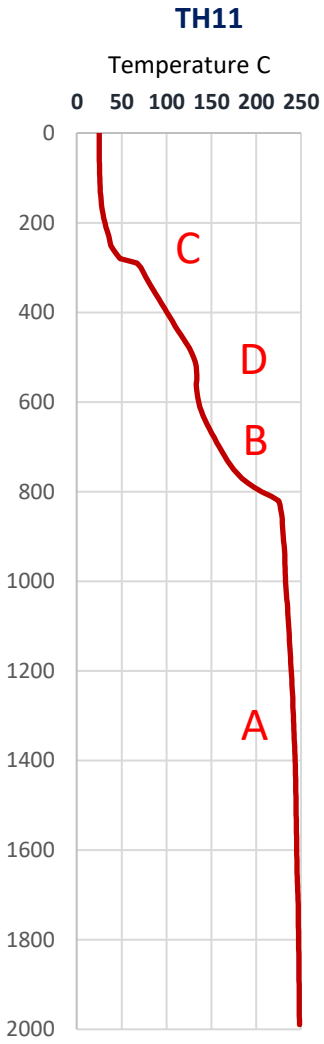

TH11: Anomaly

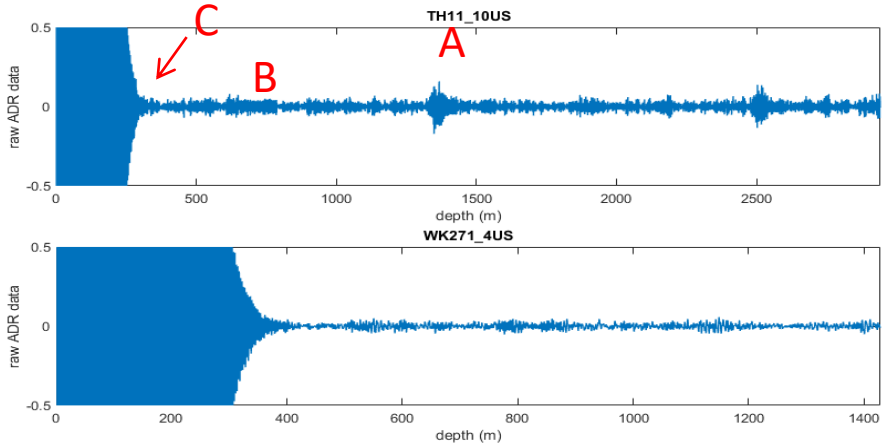

Most prominent ADR feature below 2200m is at 1320-1420m (A), which does not correspond with a temperature change. The B "burst" from 600-790m corresponds to a marked steep raise in temperature. The jump in temperature at 280m perhaps can be seen at C at 305m in the ADR plot, but it is too close to the saturation zone to be sure.

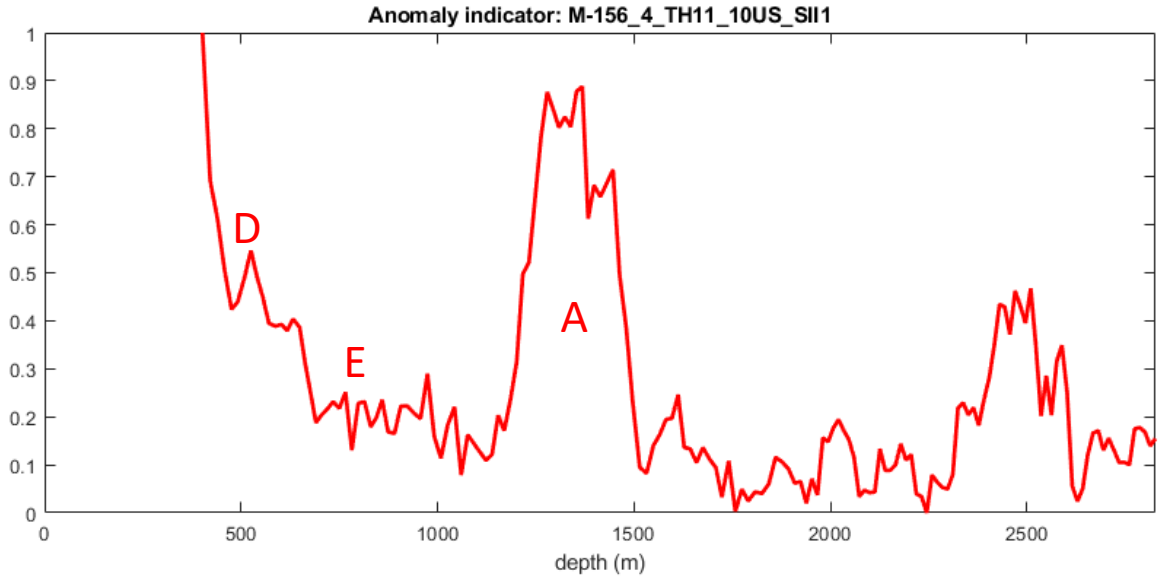

Anomaly was computed over a sliding 8192 window. The kink at D is visible. The anomaly then drops and at E it stays low, indicating "normal" behaviour. This fits nicely with the flattening out of the temperature curve from E on. The large anomaly at A (present in all data) is seen again (as is the other one at 2500m as in the other data, but I don't consider it since it's below the temperature log range).

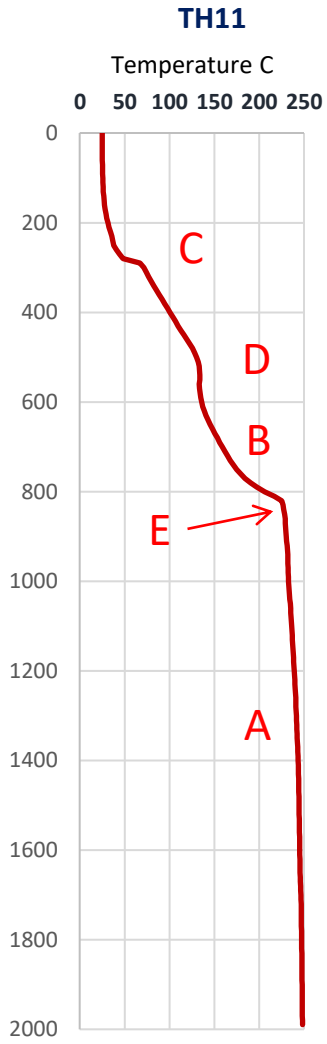

WK271: Raw data

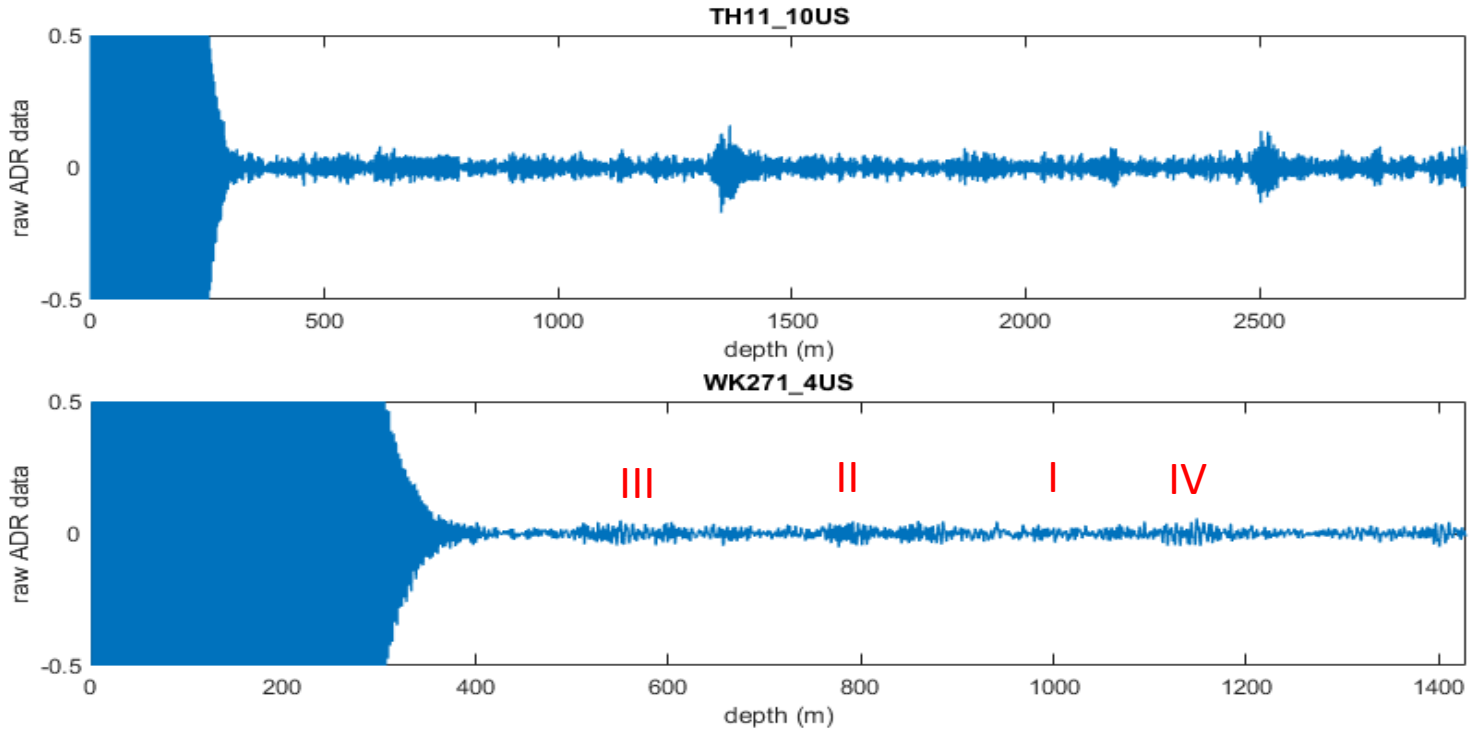

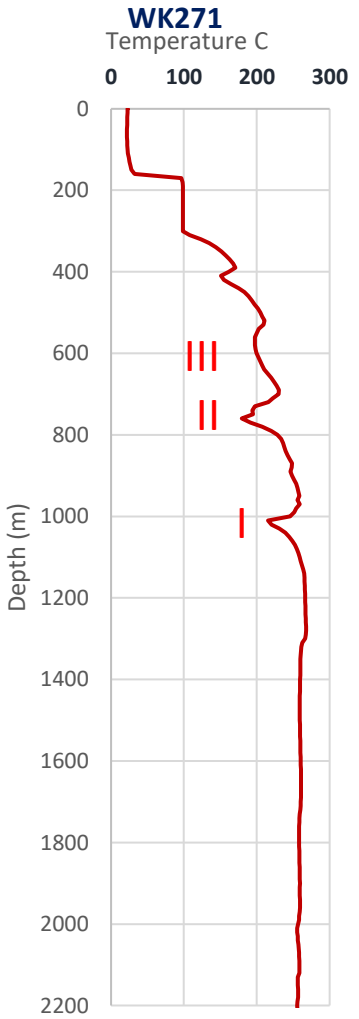

Working back from features in the T logs. Dip at 1000m (I) invisible in ADR raw. Dip near 800m (II) is accompanies by a burst in ADR data. Feature III shows a long ADR burst ~500-600m. The burst IV does not seem to be caused by temperature effects, unless it's the tiny kink indicated.

WK271: Correlation/entropy

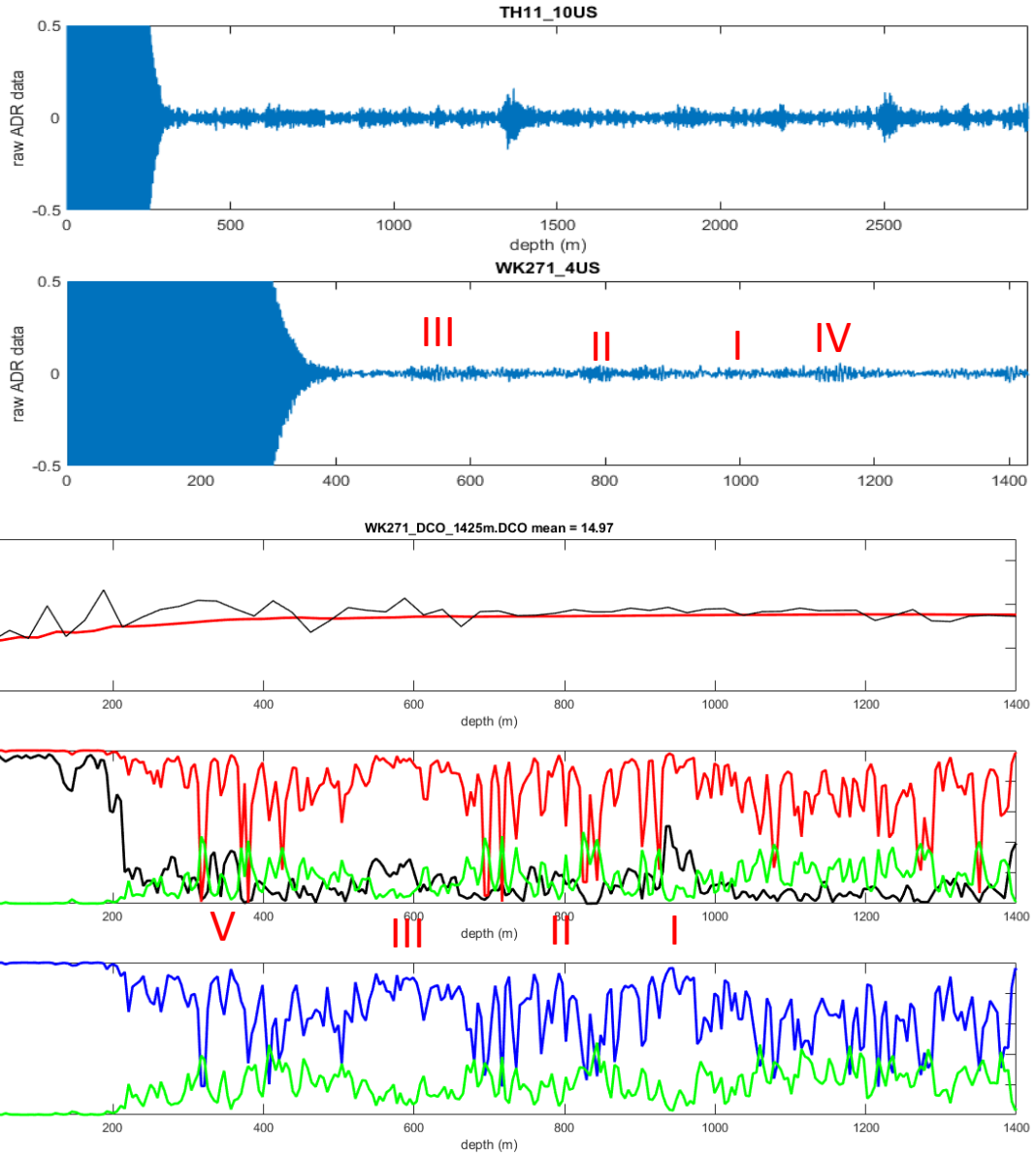

Working back from features in the T logs. Dip at 1000m (I) invisible in ADR raw. Dip near 800m (II) is accompanies by a burst in ADR data. Feature III shows a long ADR burst ~500-600m. The burst IV does not seem to be caused by temperature effects.

Correlation/entropy seems very high. The red correlation (and blue entropy) staying up so high all the time usually indicated equipment malfunctioning, but examining the QAQC data (including audio) reveals no problems. Because again correlations are strong enough that the raw correlations (black) suffice and the more involved Monte Carlo based correlation and entropy are overkill here.
Apart from confirming results from the raw data analysis, the peak at V corresponds to the sudden raise in temperature between 300 and 400m. The anomaly at "I" is too shallow in the correlation by about 100m.

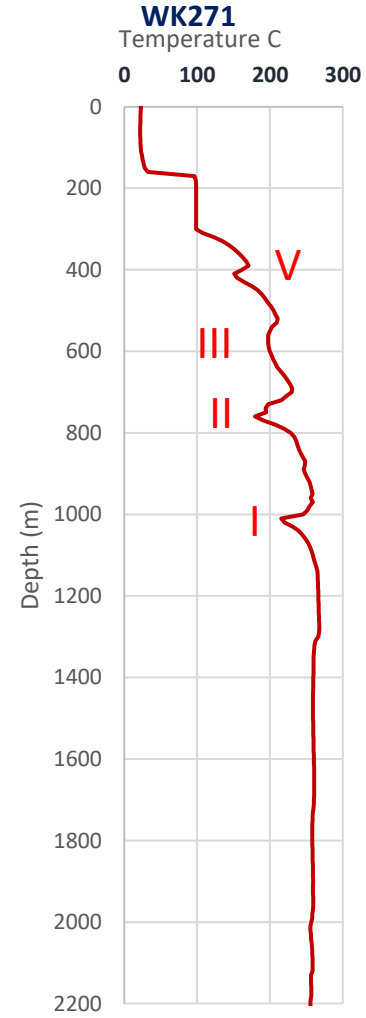

WK271: Anomaly

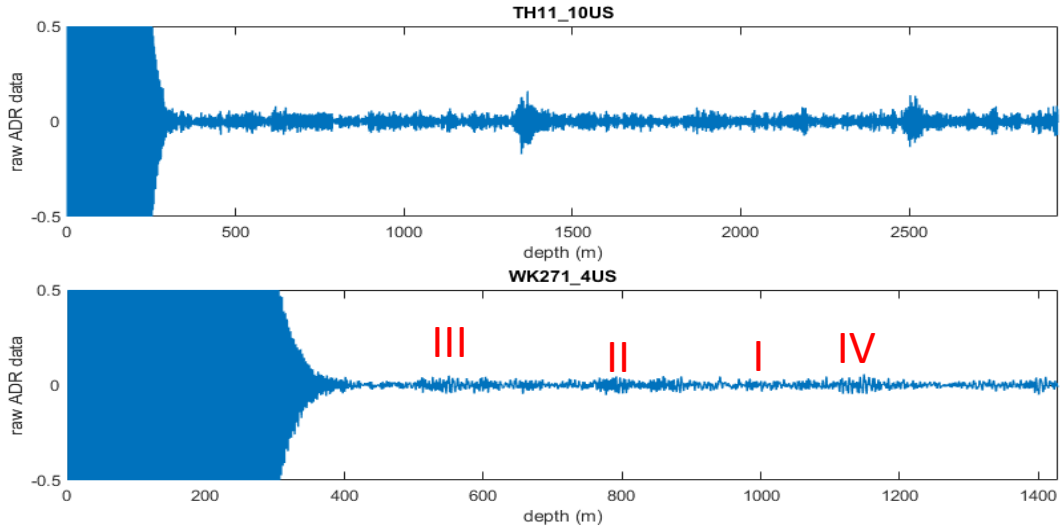

Working back from features in the T logs. Dip at 1000m (I) invisible in ADR raw. Dip near 800m (II) is accompanies by a burst in ADR data. Feature III shows a long ADR burst ~500-600m. The burst IV does not seem to be caused by temperature effects.

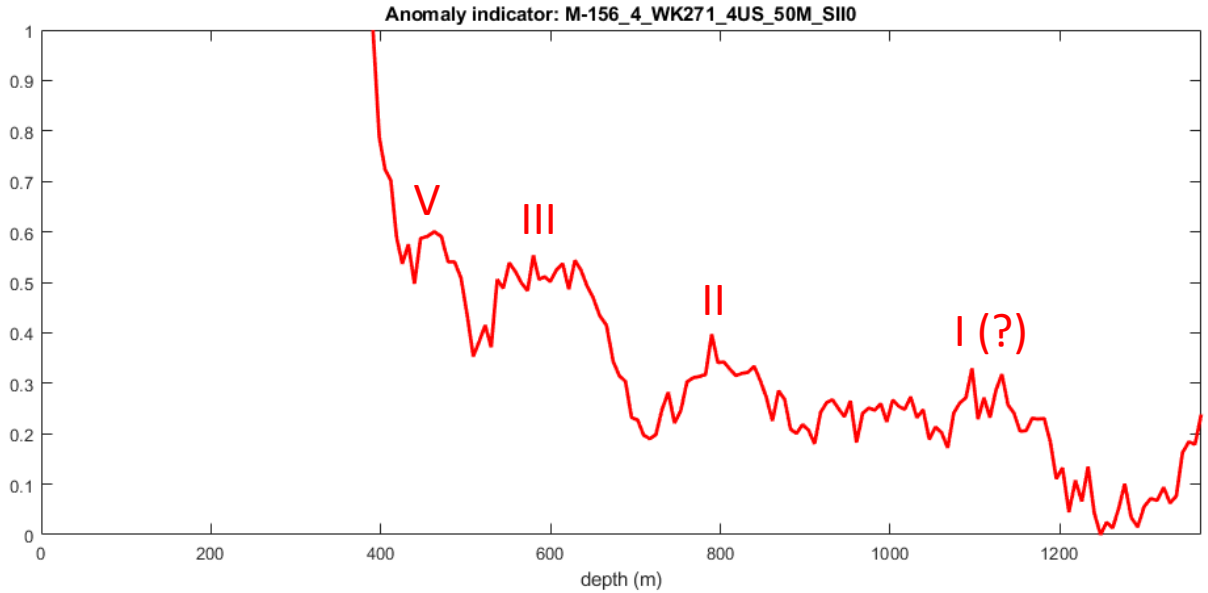

Anomaly was computed over a sliding 8192 window. The features II, II, and V are clear from the anomaly plot, the bottom feature "I" at 1km depth is again off by about 100m, but now it's too deep.

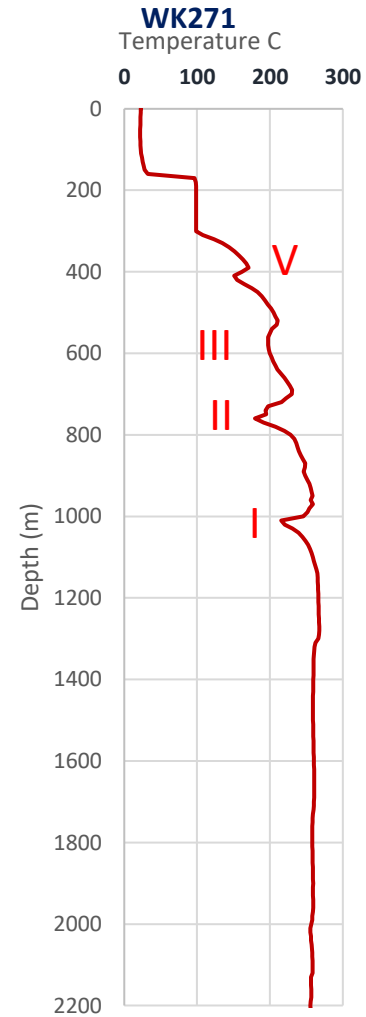

Conclusions & Recommendations

- Adrok has re-analysed the E-Gamma results for TH11 and WK271 focussing only on the 40 lowest E-Gamma values. These were compared with temperature data provided by Contact Energy.
- Adrok's dielectric constant data has also been compared against the same dataset.
- From these results Adrok concludes the following:

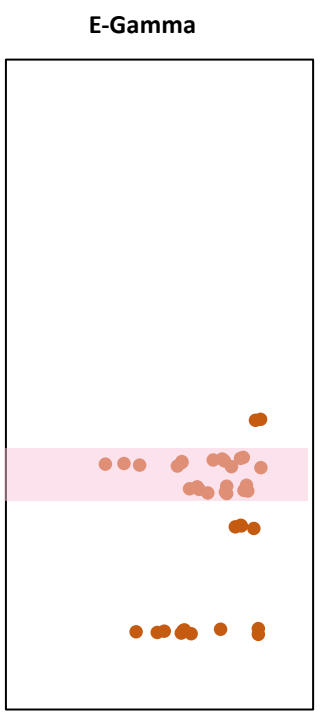

When you see this

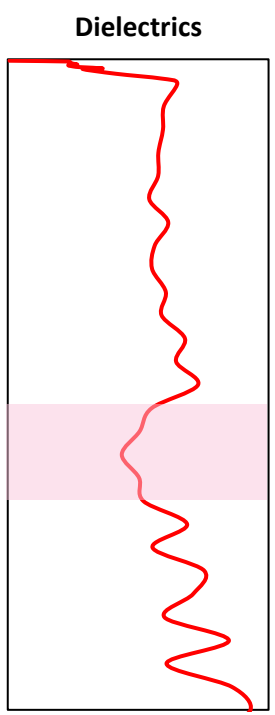

Or you see this

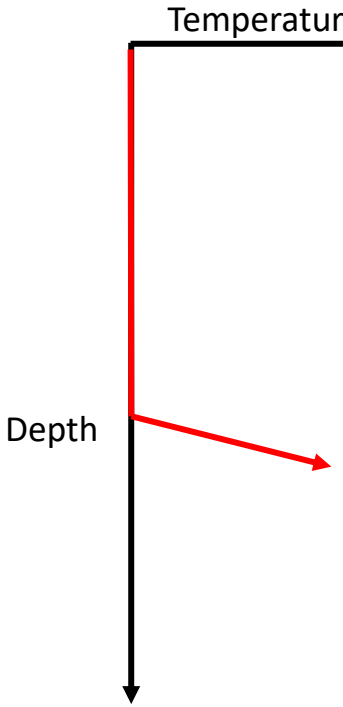

The down hole temperature is doing this

The next steps for this project are to scan more sites and increase the dataset in order to refine the procedures developed.

/… Conclusions & Recommendations

- It was shown that raw data plot, correlation/entropy and anomaly curves show features in temperature curves.
- Consistent with neural net simulations from Kern river where these processed variables produced reasonable temperature blind predictions, but E_γ remains the primary indicator
- Recommend to add anomaly to ADR analysis toolkit
  - It gives quick “at a glance” view of the main features in the data
  - It will require some “tuning” of settings which can only be determined from practice
  - Current SDK utility needs a few tweaks before G&G deployment (2-3 days work max)
- Motivation of methods such as DL provides on slide 3 is very important to get client confidence. One could argue though that water evaporation is not (the only) physics going on here as pure water itself also experiences a drop in dielectric when heated without any evaporations.

Summary of geothermal applications

- Pulsed electromagnetic ADR waves can identify change in temperature using dielectrics, conductivity and energy reflections from return signals.
- Case Studies presented from onshore UK & New Zealand.
- The field measurements show encouraging potential for the technology to be applied as a pre-drilling tool in onshore geothermal plays around the world, given the ease of survey deployment and low environmental footprint.

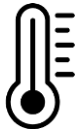

Measuring Temperature

The principal application for Adrok would be in the pre-drilling terrain- to prospect-scale thermal characterisation of the crust. Thermal maps could be easily generated which point towards the best target areas.

Adrok requires some calibration work before providing absolute values.

Measuring Water

Water has a high dielectric (>80). Due to this natural feature, the pulsed EM can measure peaks in relative dielectric values with depth.The identification of water-rich/aquifer layers at depth could be targeted in a similar way to the lithium brines in fracture hosted fluid pathways in Cornwall.

Monitoring temperature

Adrok can be used at key location around a geothermal borehole for example to monitor the change in temperature over time. If survey stations are established, ADR measurements could be made from the same station 12 months apart to provide a guide as to the annual change in temperature.This can, in turn, be used to better forecast the longevity of a geothermal field.

Useful in built up areas

Adrok is the only known technique that can directly target thermal anomalies in cities and towns where anthropogenic sources are often disruptive to other EM techniques for example.The ADR tool uses lower energy and several scans have been carried out in the middle of towns, on the sides of roads or even in the remote jungles! The portability and ease of manipulation of the equipment means it is very user friendly, cheap and non-invasive. NO SPECIAL PERMITS ARE REQUIRED!

Selected Publications

1. van den Doel, K., Jansen, J., Robinson, M., Stove, G.C. and Stove, G.D.C.,Ground penetrating abilities of broadband pulsed radar in the 1-70MHz range. In: SEG Technical Program Expanded Abstracts 2014, Denver. 1770–1774.
2. van den Doel, K. and Stove, G., Modeling and Simulation of Low Frequency Subsurface Radar Imaging in Permafrost. Computer Science and Information Technology, 2018 6(3), 40–45.
3. Stove, G. and van den Doel, K., Large depth exploration using pulsed radar. In: ASEG-PESA,Technical Program Expanded Abstracts 2015, Perth. 1–4.
4. Stove, G. D. C., Stove, G.C., and Robinson, M., 2018, New method for monitoring steam injection for Enhanced Oil Recovery (EOR) and for finding sources of geothermal heat. Australasian Exploration Geoscience Conference 2018 (AEGC), Sydney.
5. van den Doel, K. and Stove, G., Calculation of Optimal Noise Levels for the Detection of Conductive Lenses in Permafrost with Radar Scans, 81st EAGE Conference and Exhibition 2019 (1), 1-5.
6. van den Doel, K., Modeling and Simulation of a Deeply Penetrating Low Frequency Subsurface Radar System, 78th EAGE Conference and Exhibition 2016.
7. van den Doel, K. and Robinson, M., Numerical Simulation of Aquifer Detection Using Low Frequency Pulsed Radar, PIERS 2015, Prague.
8. Stove, G., 2018, Extending the reach of radio waves for subsurface water detection, CSEG Recorder,Vol. 43 No.06, pp 26-30
9. Stove, G., 2020, Helping De-Risk the Exploration for Suitable Geothermal Drill Targets, Geothermal Rising / Geothermal Resources Council (GRC) 2020 Annual Meeting
10. van den Doel, K, Robinson M, Stove C, Stove G., 2020, Subsurface Temperature Measurement Using Electromagnetic Waves and Machine Learning for Enhanced Oil Recovery, Conference Proceedings, 82nd EAGE Annual Conference & Exhibition, Volume 2020, p.1 – 5

Become part of the solution

ECONOMICAL

We will be reducing exploration costs by up to 90%

CONVENIENT

Faster solution eliminating the need for exploratory drilling

ENVIRONMENTALLY FRIENDLY

Harms the environment in no way

Gordon Stove
CEO & Co-founder

Adrok®

+44(0)131 555 6662
+44(0) 7939 051 829
gstove@adrokgroup.com
www.adrokgroup.com

Follow Us:

Adrok Ltd. 49-1 West Bowling Green Street Edinburgh, EH6 5NX, SCOTLAND, U.K.
Company reg. no. SC181158 | Predrilling Virtual Logging ® | Its Less Boring with Adrok ®